

# Superhumps, Magnetic Fields and the Mass-ratio in AM Canum Venaticorum

K. J. Pearson<sup>★</sup>

*Louisiana State University, Department of Physics and Astronomy, Nicholson Hall, Baton Rouge, LA 70803-4001, USA.*

Accepted . Received ; in original form

## ABSTRACT

We show that the observed  $K$  velocities and periodicities of AM CVn can be reconciled given a mass ratio  $q \approx 0.22$  and a secondary star with a modest magnetic field of surface strength  $B \sim 1$  T. We see that the new mass ratio implies that the secondary is most likely semi-degenerate. The effect of the field on the accretion disc structure is examined. The theory of precessing discs and resonant orbits is generalised to encompass higher order resonances than 3:2 and shown to retain consistency with the new mass ratio.

**Key words:** accretion, accretion discs – binaries: close – methods:  $N$ -body simulations – MHD – stars: individual: AM CVn – novae, cataclysmic variables

## 1 INTRODUCTION

AM CVn is the prototype of a helium-rich class of ultra-short period Cataclysmic Variable (CV) binaries. The eleven member systems consist of a white dwarf primary accreting material, through Roche lobe overflow, from a companion star that is itself degenerate or semi-degenerate. Nelemans et al. (2001a) recognised two formation scenarios for these systems. The “white dwarf family” arise from detached double degenerate white dwarf binaries that evolved into contact through gravitational wave radiation (Faulkner, Flannery & Warner 1972). The “helium star family” arise from systems where a low-mass helium-burning secondary is brought into contact, again through gravitational wave radiation. Once mass transfer has reduced  $M_2 < 0.2M_\odot$ , core helium burning ceases and the star becomes semi-degenerate (Savonije, de Kool & van den Heuvel 1986; Iben & Tutukov 1991).

Seven of the known AM CVn stars, including the prototype, show periodicities in addition to their orbital modulations that are generally interpreted as arising from a precessing, non-axisymmetric, accretion disc. Several of the members show regular dips in brightness on a timescale of a few days. This suggests a similar phenomenon to the disc thermal instabilities in dwarf novae (Smak 1983; Cannizzo, Shafter & Wheeler 1988; Tsugawa & Osaki 1997) albeit with a helium rather than hydrogen dominated disc. Dwarf novae show regular outbursts where the luminosity increases by 2–5 magnitudes and a subset also show “superhumps” caused by a precessing accretion disc. Here, though, the default state appears to be “high”: ie. one in which helium

is ionized and the disc has a high viscosity. At some point the disc drops below a critical temperature, helium recombines and the disc switches to a low viscosity state. Material collects in the accretion disc and switches back to the high state at a second, critical temperature. These critical temperatures are normally converted to equivalent critical surface densities  $\Sigma_{\text{crit}}$ . Exceptions are AM CVn itself, that has never been observed to dip, and GP Com which appears to be in a permanent low state (Warner 1995).

Nelemans, Steeghs & Groot (2001b) examined observations of AM CVn in detail and arrived at a definite identification of  $P_{\text{orb}} = 1028.73$  s. Using the beat period,  $P_b = 13.38$  h, standard precessing disc theory gives a mass ratio for the system  $q = 0.087$ . However, their measurements of the HeII 4286 Å line suggested  $K_1 = 53 \pm 6$  km s<sup>-1</sup> which, coupled with  $K_2 = 210$ –280 km s<sup>-1</sup>, indicate a mass ratio in the range  $0.19 < q < 0.25$ . The authors noted the inconsistency implicit here and chose to rely on the commonly used mass-ratio inferred from disc theory. They also noted the alternative that the usual precession  $P_b$ - $P_{\text{orb}}$ - $q$  relation (given later in equation (12)) might be inappropriate.

The purpose of this paper is to reconcile these two methods of determining  $q$  by proposing that a modest secondary magnetic field is present in AM CVn. We suggest that the true AM CVn mass ratio is that derived directly from the  $K$  velocities and that the widely accepted  $P_b$ - $P_{\text{orb}}$ - $q$  relation used by Nelemans, Steeghs & Groot (2001b) is indeed inappropriate in this case.

Pearson, Wynn & King (1997) studied the effect of a secondary’s field on the behaviour of dwarf novae: placing upper limits of  $B_{L1} < 0.16$  T ( $\mu_2 \lesssim 7 \times 10^{34}$  G cm<sup>3</sup>) in U Gem and  $B_{L1} < 0.023$  T ( $\mu_2 \lesssim 4 \times 10^{32}$  G cm<sup>3</sup>) in Z Cha. They

<sup>★</sup> Send offprint requests to: kjp1@rouge.phys.lsu.edu

found that stronger fields had the effect of shrinking the disc radius and of exciting resonances in the disc. However, the disc was too small to access the 3:2 resonance normally observed in superhumping systems and instead higher order resonances appeared. These higher resonances are available, in principle, to all CV accretion discs that do not reach the required 3:2 resonant radius, even in the absence of a secondary field. However, in practice, the tidal effect that drives the superhump resonance is unable to excite the higher orders before they are damped out by viscosity. It is the addition of the secondary field that enables these higher resonances to be excited and their appearance or otherwise that enables us to constrain the secondary's magnetic field strength. We would expect a secondary with a magnetic field in AM CVn to have a similar effect: ie. to shrink the disc, excite higher order resonances and to thereby alter the applicable  $P_b$ - $P_{orb}$ - $q$  relation.

It has long been problematic to understand the origin of the magnetic field in the secondaries of CVs: particularly those systems that lie below the 2–3 hr “period gap” where the stars are fully convective. However, we know that such a field must be possible, if not ubiquitous, from the fact that the Polars are able to lock in synchronous rotation through the interaction of the two stellar dipoles. This locking requires that the secondary has a magnetic moment  $\mu_2 \sim 10^{33}$ – $10^{34}$  G cm<sup>3</sup> (King, Whitehurst & Frank 1990) that is similar to that of the primary. Observationally, results from a variety of open clusters (Jones, Fischer & Stauffer 1996; Stauffer et al. 1997; Terndrup et al. 2000; Reid & Mahoney 2000) suggest that the rate of magnetic braking does not reduce abruptly when stars become fully convective ( $M \lesssim 0.3M_\odot$ ); implying the continued presence of a significant magnetic field. Such a field also has implications for the standard model of the period gap that relies on the rate of magnetic braking dropping sharply at the upper end (Andronov, Pinsonneault & Sills 2003).

Recently, models have begun to emerge for the generation of magnetic fields by fully convective, rapidly rotating, young stars (Küker & Rüdiger 1999) that may survive as relics into the main sequence lifetime (Kitchatinov, Jardine & Collier Cameron 2001). These fields are non-dipolar and highly non-axisymmetry. Such geometries, if repeated in fully convective CV secondaries, may have interesting consequences for the equilibrium alignment of Polars and the interpretation of the “hot spot” to which material is channelled at the white dwarf surface. These models, however, have not so far extended into the extremely rapid rotation regime required for CV secondaries; especially with as short a  $P_{orb}$  as AM CVn. We are also confronted, in this particular case, with a secondary that is at least semi-degenerate with the unknown consequences for the field that such a structure and previous evolution will have. However, since for a dipolar field  $f \propto B^2 \propto r^{-6}$ , it would require a relatively much weaker dipole moment to achieve the same local field strength in these short period, small separation systems than in wider long period CVs. It is, therefore, not unreasonable to expect to see effects in these systems that might not be apparent in their longer period counterparts.

In section 2 we outline the important background theory to the problem; generalising the theory of superhump resonances to higher orders in section 2.1 and deriving com-

ponent masses for the system in section 2.2. We describe simulations of the system in section 3.

## 2 THEORETICAL BACKGROUND

### 2.1 Predicting Superhump Periods

Hirose & Osaki (1990) derived the general expression for the ratio of the disc precession  $\omega_p$  and orbital  $\omega_{orb}$  frequencies in terms of the mass ratio and radius of disc material. Their equation (8) is

$$\frac{\omega_p}{\omega_{orb}} = \frac{q}{(1+q)^{\frac{1}{2}}} \left[ \frac{1}{2r^{\frac{1}{2}}} \frac{d}{dr} \left( r^2 \frac{dB_0}{dr} \right) \right], \quad (1)$$

where

$$B_0(r) = \frac{1}{2} b_{\frac{1}{2}}^0 = F \left( \frac{1}{2}, \frac{1}{2}, 1, r^2 \right) \quad (2)$$

(Brumberg 1995) is the zeroth order Laplace coefficient given in terms of the hypergeometric function  $F$ ,  $q = M_2/M_1$  ( $< 1$ ) is the mass-ratio and  $r$  is the radius of orbiting material expressed as a fraction of the separation  $a$ . Writing the hypergeometric function in its series form

$$F \left( \frac{1}{2}, \frac{1}{2}, 1, r^2 \right) = \sum_{n=0}^{\infty} \frac{\left(\frac{1}{2}\right)_n \left(\frac{1}{2}\right)_n}{(1)_n n!} r^{2n} \quad (3)$$

$$= 1 + \frac{1}{4}r^2 + \frac{9}{64}r^4 + \dots + C_n r^{2n}. \quad (4)$$

The coefficients are calculable exactly but rapidly become unwieldy with large numerators and denominators. However, after some algebra we can rewrite the general expression for them as

$$C_n = \left[ \frac{(1)(3)(5)\dots(2n-1)}{n!2^n} \right]^2 \quad (5)$$

$$= \prod_{m=1}^n \left( \frac{2m-1}{2m} \right)^2, \quad (6)$$

which at least clears away the less transparent fractional terms in Pochhammer's symbol of  $\left(\frac{1}{2}\right)_n$ . Combining equations (1), (4) and (6), and after some more algebra and a little differentiation, we can arrive at a general relation for resonant orbits

$$\frac{\omega_p}{\omega_{orb}} = \frac{3}{4} \frac{q}{(1+q)^{\frac{1}{2}}} r^{\frac{3}{2}} \left[ 1 + c_2 r^2 + c_3 r^4 + c_4 r^6 + \dots + c_n r^{2(n-1)} \right], \quad (7)$$

where the coefficients are related by

$$c_n = \frac{2}{3}(2n)(2n+1)C_n. \quad (8)$$

The values of  $C_n$  and  $c_n$  up to  $n = 5$  are listed in Table 1 for convenience.

The radii of resonant orbits is given by Frank, King & Raine (1992). Restricting ourselves to the case of  $j:j-1$  resonances, that are strongest, we obtain

$$r_j = \frac{1}{j^{\frac{2}{3}}(1+q)^{\frac{1}{3}}}. \quad (9)$$

$n$	0	1	2	3	4	5
$C_n$	1	$\frac{1}{4}$	$\frac{9}{64}$	$\frac{25}{256}$	$\frac{1225}{16384}$	$\frac{3969}{65536}$
$c_n$	0	1	$\frac{15}{8}$	$\frac{175}{64}$	$\frac{3675}{1024}$	$\frac{72765}{16384}$

**Table 1.** Coefficients contained in the expansions defined in equations (6) and (8) up to  $n = 5$ .

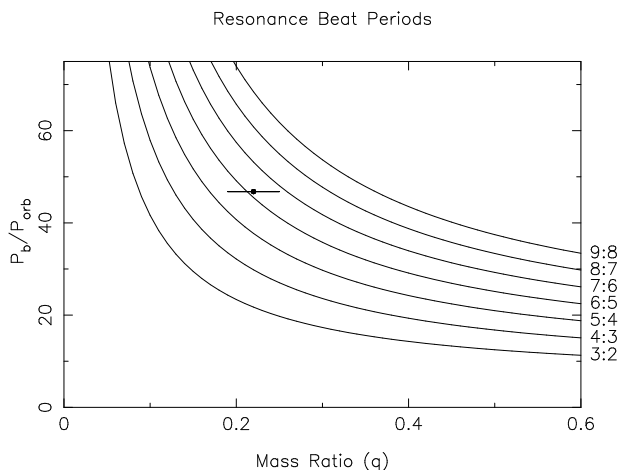


**Figure 1.** Relation between the precession to orbital beat period and mass ratio given in equation (11) for different resonances  $j:j-1$ . Also indicated is the range of the mass ratio allowed by  $K$  velocity measurements for AM CVn.

Thus we finally arrive at

$$\frac{\omega_p}{\omega_{orb}} = \frac{3}{4j} \frac{q}{1+q} \left[ 1 + \frac{c_2}{j^{\frac{4}{3}}(1+q)^{\frac{2}{3}}} + \frac{c_3}{j^{\frac{8}{3}}(1+q)^{\frac{4}{3}}} + \frac{c_4}{j^4(1+q)^2} + \frac{c_5}{j^{\frac{16}{3}}(1+q)^{\frac{8}{3}}} + \dots \right]. \quad (10)$$

Since these are resonant orbits, the (long) beat period is related to the orbital and precession angular frequencies by

$$P_b = P_{orb} \frac{j}{j-1} \frac{\omega_{orb}}{\omega_p}. \quad (11)$$

This is plotted for several resonances in Figure 1. The familiar approximation

$$P_b = A \frac{1+q}{q} P_{orb}, \quad (12)$$

where  $A \approx 3.85$  for  $0.1 < q < 0.22$  (Warner 1995), is recovered by setting  $j = 3$  and evaluating the term in square brackets in (10) with  $q = 0.16$ . The limiting mass ratio  $q \approx 0.22$  found by Whitehurst (1988a) arises from the largest value for which  $r_3$  remains within the last stable stream line (Molnar & Koblunicky 1992).

We can derive parallel approximations to (12) for other resonances in a similar way. The coefficient  $A$  need only be recalculated with the appropriate value of  $j$ . Table 2 gives  $A$  for different values of  $j$ ; appropriate again to the range  $0.1 < q < 0.22$  by evaluating with  $q = 0.16$ .

For the particular case of AM CVn, using  $q = 0.22$  the full expressions give rise to the predicted superhump periods and disc radii shown in Table 3.

$j$	3	4	5	6	7	8	9
$A$	3.86	5.33	6.75	8.16	9.55	10.9	12.3

**Table 2.** Coefficient  $A$  contained in the approximation (12) for several resonances and appropriate to  $0.1 < q < 0.22$ .

Resonance ( $j : j - 1$ )	Radius ( $r_j$ )	$\frac{P_b}{P_{orb}}$
3 : 2	0.450	21.8
4 : 3	0.371	29.8
5 : 4	0.320	37.7
6 : 5	0.283	45.5
7 : 6	0.256	53.2
8 : 7	0.234	60.8
9 : 8	0.216	68.4

**Table 3.** The radius and beat period of superhump resonances for  $q = 0.22$ .

## 2.2 Mass Determinations

We can write the approximation by Eggleton (1983) for the size of the secondary's Roche lobe as

$$R_2 = \left[ \frac{G}{4\pi^2} \right]^{\frac{1}{3}} \frac{0.49q^{\frac{1}{3}}(1+q)^{\frac{1}{3}}}{0.6q^{\frac{2}{3}} + \ln(1+q^{\frac{1}{3}})} M_2^{\frac{1}{3}} P_{orb}^{\frac{2}{3}}, \quad (13)$$

where we have eliminated  $a$  using Kepler's Third Law. Knowing  $P_{orb}$  and  $q$ , for a given mass-radius relation we can eliminate  $R_2$  and solve for  $M_2$ .

For a fully degenerate He white dwarf secondary, the relation

$$\frac{R}{R_{\odot}} \approx 0.0106 - 0.0064 \ln \left( \frac{M}{M_{\odot}} \right) + 0.0015 \left( \frac{M}{M_{\odot}} \right)^2 \quad (14)$$

(Zapolsky & Salpeter 1969; Rappaport & Joss 1984) is appropriate. For a semi-degenerate secondary, the relation is more problematic. However, approximations of the form

$$\frac{R}{R_{\odot}} \approx b \left( \frac{M}{M_{\odot}} \right)^{-\alpha} \quad (15)$$

have been found by Tutukov & Fedorova (1989) with  $b = 0.043$ ,  $\alpha = 0.062$  (hereafter 'TF' parameters) and Savonije, de Kool & van den Heuvel (1986) with  $b = 0.029$ ,  $\alpha = 0.19$  (hereafter 'SKH'). The resulting values for  $M_1$  and  $M_2$  are listed in Table 4 for each case.

Secondary Type	$M_1/M_{\odot}$	$M_2/M_{\odot}$
Degenerate	0.156	0.034
Semi-degenerate (TF)	0.529	0.116
Semi-degenerate (SKH)	0.418	0.092

**Table 4.** Derived values for the AM CVn component masses assuming  $q = 0.22$  and different mass-radius relations for the secondary.

Nelemans et al. (2001a) carried out a population synthesis study of AM CVn systems. They noted that the previously adopted  $q = 0.087$  gave rise to component masses that were difficult to reconcile with their results. For a degenerate secondary and that mass ratio, the system would lie at the low end of the predicted distribution and for a semi-degenerate system would imply a primary mass close to, if not in excess of, the Chandrasekhar mass. Locating the results from Table 4 on their Figure 1, we see that for  $q = 0.22$  and a fully degenerate secondary, the system would have to have been born at an implausibly unlikely position in the tail of the distribution. For a semi-degenerate secondary, however, the difficulties of a very high  $M_1$  have now been resolved with a more comfortable  $M_1 \sim 0.5M_\odot$ .

### 3 SIMULATIONS

Modelling was carried out using the same code HYDISC (Whitehurst 1987; Whitehurst 1988b) used originally to demonstrate the tidal origin of superhump resonances (Whitehurst 1988a). It has since been adapted to a variety of other CV (Wynn & King 1995; Wynn, King & Horne 1997; King & Wynn 1999) and young star (Pearson & King 1995; Ultchin, Regev & Wynn 2002) applications. The modifications necessary to include a secondary magnetic field were discussed in Pearson, Wynn & King (1997).

Simulations of the effect of the secondary field in CVs were recently reexamined by Murray et al. (2002) using SPH. These authors modelled the magnetic interaction through an acceleration

$$\mathbf{a} = -k[\mathbf{v} - \mathbf{v}_f]_\perp, \quad (16)$$

where  $\mathbf{v}$  and  $\mathbf{v}_f$  are the velocities of the material and field lines respectively and  $\perp$  indicates that only components perpendicular to the field lines are considered. Such a form, originating from models that used a diamagnetic prescription for the interaction, can also be applied to more general forms. In that case, our ignorance of the details of the interaction are contained in  $k$  and, in particular, in its behaviour as a function of position and magnetic field strength. We prefer here to retain the model of the interaction contained in Pearson, Wynn & King (1997). That is, that the disc is assumed to wind up the magnetic field through advection until  $B_\phi \sim B_z$  (Aly & Kuijpers 1990; Wang 1996). This enables us to maintain an explicit relationship between the force and secondary field strength. Specifically, this earlier study showed that the acceleration experienced by each particle could be modelled as

$$\mathbf{a} = -\frac{2\pi B^2 R \Delta R}{\mu_0 \beta N m_p} \mathbf{e}_\phi \quad (17)$$

where  $m_p$  is the mass represented by each particle,  $N$  is the number of particles in a bin of width  $\Delta R$  at a distance  $R$  from the white dwarf,  $B$  is the local magnetic field strength and  $\beta$  is a dimensionless parameter related to the exact geometry of the field distortion (set equal to unity hereafter). Since we have a strong constraint in the superhump period, we can place limits on the possible secondary field strength.

The secondary's magnetic field acts on the disc material in a similar way to the gravitational tidal interaction. However, the disc material is now coupled more strongly

to the secondary by the field. As a result, the disc needs to find a new configuration where the outward advection of angular momentum can meet the more efficient transfer back to the secondary. The  $B^2 \propto r^{-6}$  dependence provides a sharp “spike” to the interaction that acts to promote the appearance of resonance phenomena. There is a limiting field strength below which the disc can find a suitable new structure. Above this, angular momentum extraction is too efficient, the disc is completely disrupted and material is rapidly accreted by the primary.

We adopted the system orbital period of 1028.7 s confirmed by Nelemans, Steeghs & Groot (2001b), the mass ratio  $q = 0.22$  in the middle of the range implied by the  $K$  velocities and  $M_1 = 0.5M_\odot$ .

Each simulation was started with a burst of particles over an initial  $2P_{\text{orb}}$  before being reduced to a steady 90 per orbit. The magnetic interaction was “switched on” after  $3P_{\text{orb}}$  once a disc had begun to form. Each of the simulations was allowed to run for at least  $500P_{\text{orb}}$ , allowing an equilibrium to be reached.

We can estimate the effective value of the Shakura-Sunyaev parameter  $\alpha$  from the ring of material that forms initially at the circularization radius  $R_c$  in a non-magnetic simulation. Ignoring any additional mass transfer of material, the surface density  $\Sigma$  of an initial ring of mass  $m$  will evolve as

$$\Sigma(x, \tau) = \frac{m}{\pi R_c^2} \tau^{-1} x^{-\frac{1}{4}} \exp\left\{-\frac{(1+x^2)}{\tau}\right\} I_{\frac{1}{4}}\left(\frac{2x}{\tau}\right) \quad (18)$$

(Frank, King & Raine 1992) where  $x = R/R_c$ ,  $I$  is a modified Bessel function and  $\tau = 12\nu t R_c^{-2}$ . Fitting this to the early time behaviour where the much lower “steady state” mass transfer has negligible effect gives a viscosity  $\nu \approx 6.1 \times 10^8 \text{ m}^2 \text{ s}^{-1}$ . From a Gaussian fitted to the vertical disc profile we have a scale height  $H \approx 1.2 \times 10^5 \text{ m}$ . Hence, using a sound speed appropriate to a fully ionized gas of solar abundance at  $\sim 10^4 \text{ K}$ , we derive  $\alpha \sim 0.3$ .

The particle mass used in the magnetic interaction (17) was determined from a nominal mass transfer rate of  $10^{14} \text{ kg s}^{-1}$ . However, as the particles have negligible mass gravitationally, this is the only place in which  $m_p$  appears in the equations of motion. Thus the magnetic simulations may be characterised by the parameter  $\frac{B^2}{M_2}$ . We use the  $L_1$  point as the fiducial position for the surface strength of the secondary's field and assume the field strength to vary as for a dipole.

In common with Pearson, Wynn & King (1997) and Murray et al. (2002), we see that the magnetic field tends to shrink and promote resonant behaviour in the disc (see eg. Figure 2) although the resonances are relatively weak compared to SU UMa superhumps. Simulations with  $B_{L1} \lesssim 0.5 \text{ T}$  are unable to excite any resonances. Similarly, when  $B_{L1} \gtrsim 1 \text{ T}$  the disc is completely disrupted. Surface density profiles are shown in Figure 3 for different magnetic field strengths. The critical surface densities for “dwarf nova” type thermal instabilities in helium discs are taken from Tsugawa & Osaki (1997) using a hot state  $\alpha = 0.3$  and cold state  $\alpha = 0.03$ . We see that all the “magnetic” discs have surface densities between the two critical values and, hence, that they can maintain either a “hot” or “cold” state. However, the effective value of  $\alpha$  derived above implies that the simulations represent a “hot” disc configuration which

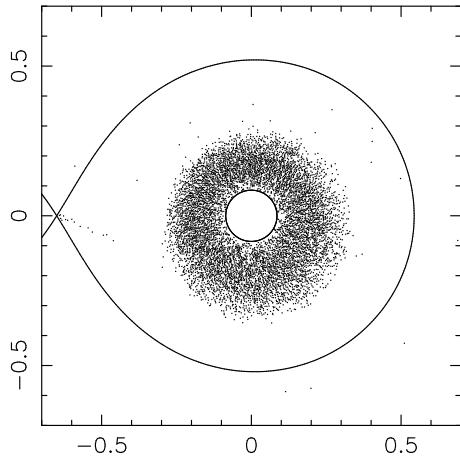


**Figure 2.** Particle distribution for the  $B_{L1} = 0.7$  T simulation showing the precessing, elliptical disc pattern.

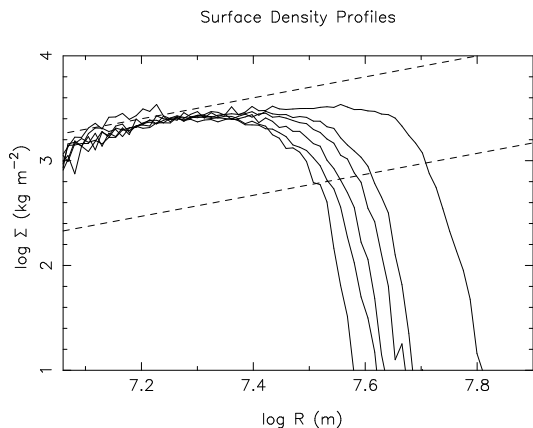


**Figure 3.** Mean surface density profile for equilibrium simulations with  $B_{L1} = 0, 0.6, 0.65, 0.7, 0.75, 0.8$  T (decreasing radius). Also shown (dashed line) are the critical surface densities for transition to the “hot” (upper line) and “cold” states.

is consistent with the observation that AM CVn is in a permanent “high” state.

We can derive the precession period of the disc by considering plots of the angular distribution of particles, such as those in Figure 4, plotted every  $P_{orb}$ . We can also use Fourier transforms of the number of particles in a particular azimuthal bin, although, even running for  $512 P_{orb}$  there is limited resolution at long  $P_b$ . These periods are summarised for each field strength in Table 5. The models bracket the observed  $P_b = 46.8 P_{orb}$  and, conservatively, place limits on the allowed field strength of  $0.65 \text{ T} < B_{L1} \left( \frac{\dot{M}_2}{10^{14} \text{ kg s}^{-1}} \right)^{-1/2} < 0.8 \text{ T}$ . These are equivalent to a magnetic moment, with the assumed mass transfer rate, of  $(6.0\text{--}7.3) \times 10^{32} \text{ G cm}^3$  which is at the low end of the range deduced for Polar secondaries. We do not quote formal errors on these limits since they are dominated by the systematic effects in our assumptions regarding the geometry of the field distortion. Pearson, Wynn & King (1997) estimated that in a worst case these values

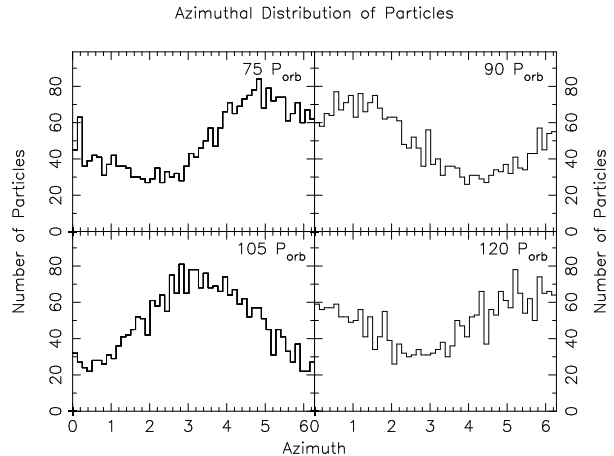


**Figure 4.** Angular distribution of particles in the disc for the  $B_{L1} = 0.7$  T simulation with  $0.225 < r < 0.325$  at  $t = 75, 90, 105, 120 P_{orb}$ . The profile can be seen to drift slowly towards higher azimuthal angles.

$B_{L1}$ (T)	0.6	0.65	0.7	0.75	0.8
$\frac{P_b}{P_{orb}}$	28	35	43	51	58
$j$	4	5	6	7	8

**Table 5.** Measured beat period and closest predicted resonance for different field strengths.

could be in error by no more than a factor 3 and were probably significantly better.

## 4 SUMMARY

We have shown that the observed  $K$  velocities in AM CVn can be reconciled with our understanding of superhump resonance behaviour given a modest secondary magnetic field. The field acts to shrink the disc and excite higher order resonances than those tidally excited in SU UMa systems. The sensitivity of the disc behaviour to the magnetic field places a tight constraint upon the possible field strength of the secondary although our errors are dominated by assumptions inherent in the model. A value of  $q = 0.22$  strongly suggests that the secondary in AM CVn is semi-degenerate and is more easily reconciled with population synthesis results than the previous  $q = 0.087$ .

We intend to return to this system in a future paper exploring more exhaustively the possible parameter space ( $M_1$ ,  $q$ ,  $B$ ,  $\nu$  etc.) which AM CVn can occupy and still reconcile the disc precession and  $K$  velocity measurements. Further direct measurements to confirm  $K_1$  would be extremely useful.

## ACKNOWLEDGEMENTS

The author would like to thank the referee Graham Wynn for his helpful remarks on the first version of the paper and

also both Juhan Frank and Keith Horne for insightful comments on a draft version. This work has been supported, in part, by the U.S. National Science Foundation through grant AST-9987344 and, in part, through LSU's Center for Applied Information Technology and Learning.

## REFERENCES

- Aly J. J., Kuijpers J., 1990, *A&A*, 227, 473  
 Andronov N., Pinsonneault M., Sills A., 2003, *ApJ*, 582, 358  
 Brumberg V. A., 1995, *Analytical Techniques of Celestial Mechanics*, Springer Verlag, Berlin  
 Cannizzo J. K., Shafter A. W., Wheeler J. C., 1988, *ApJ*, 333, 227  
 Eggleton P. P., 1983, *ApJ*, 268, 368  
 Faulkner J., Flannery B. P., Warner B., 1972, *ApJ*, 175, L79  
 Frank, J., King, A. R., Raine, D. J., 1992, *Accretion Power in Astrophysics*, Cambridge Univ. Press.  
 Hirose M., Osaki Y., 1990, *PASJ*, 42, 135  
 Iben Jr. I., Tutukov A. V., 1991, *ApJ*, 370, 615  
 Jones B. F., Fischer D., Stauffer J. R., 1996, *AJ*, 464, 943  
 King A. R., Whitehurst R., Frank J., 1990, *MNRAS*, 244, 731  
 King A. R., Wynn G. A., 1999, *MNRAS*, 210, 203  
 Kitchatinov L. L., Jardine M., Collier Cameron A., 2001, *A&A*, 374, 250  
 Küker M., Rüdiger G., 1999, *A&A*, 346, 922  
 Molnar L. A., Kobulnicky H. A., 1992, *ApJ*, 392, 678  
 Murray J. R., Chakrabarty D., Wynn G. A., Kramer L., 2002, *MNRAS*, 335, 247  
 Nelemans G., Portegeis Zwart S. F., Verbunt F., Yungelson L. R., 2001a, *A&A*, 368, 939  
 Nelemans G., Steeghs D., Groot P. J., 2001b, *MNRAS*, 326, 621  
 Pearson K. J., King A. R., 1995, *MNRAS*, 276, 1303  
 Pearson K. J., Wynn G. A., King A. R., 1997, *MNRAS*, 288, 421  
 Rappaport S. A., Joss, P. C., 1984, *ApJ*, 283, 232  
 Reid I. N., Mahoney S., 2000, *MNRAS*, 316, 827  
 Stauffer J. R., Hartmann L. W., Prosser C. F., Randich S., Balachandran S., Patten B. M., Simon T., Giampapa M., 1997, *ApJ*, 479, 776  
 Savonije G. J., de Kool M., van den Heuvel E. P. J., 1986, *A&A*, 155, 51  
 Smak J., 1983, *Acta Astron.*, 33, 333  
 Terndrup D. M., Stauffer J. R., Pinsonneault M. H., Sills A., Yuan Y., Jones B. F., Fischer D., Krishnamurthi A., 2000, *AJ*, 119, 1303  
 Tsugawa M., Osaki Y., 1997, *PASJ*, 49, 75  
 Tutukov A. V., Fedorova A. V., 1989, *SvA*, 33, 606  
 Ultchin Y., Regev O., Wynn G. A., 2002, *MNRAS*, 331, 578  
 Wang Y.-M., 1996, *ApJ*, 465, L111  
 Warner B., 1995, *Cataclysmic Variable Stars*, Cambridge Univ. Press, Cambridge  
 Whitehurst R., 1987, Ph.D. Thesis, Oxford Univ.  
 Whitehurst R., 1988a, *MNRAS*, 232, 35  
 Whitehurst R., 1988b, *MNRAS*, 233, 529  
 Wynn G. A., King A. R., 1995, *MNRAS*, 275, 9  
 Wynn, G. A., King, A. R., Horne, K. D., 1997, *MNRAS*, 286, 436  
 Zappalà H. S., Salpeter E. E., 1969, *ApJ*, 158, 809